

<https://doi.org/10.1038/s43247-025-02312-2>

Penguin guano is an important source of climate-relevant aerosol particles in Antarctica



Matthew Boyer¹ ✉, Lauriane Quéléver¹, Zoé Brasseur¹, Barry McManus², Scott Herndon², Mike Agnese², David Nelson², Joseph Roscioli², Frederik Weis³, Sergej Sel³, Giselle L. Marincovich⁴, Francisco J. Quarin⁴, Angela Buchholz⁵, Carlton Xavier⁶, Pablo J. Perchivale⁷, Veli-Matti Kerminen¹, Markku Kulmala¹, Tuukka Petäjä¹, Xu-Cheng He^{1,8}, Svetlana Sofieva-Rios^{9,10}, Hilkka Timonen¹⁰, Minna Aurela¹⁰, Luis Barreira¹⁰, Aki Virkkula¹⁰, Eija Asmi¹⁰, Doug Worsnop^{1,2} & Mikko Sipilä¹ ✉

Gaseous ammonia, while influential in atmospheric processes, is critically underrepresented in atmospheric measurements. This limits our understanding of key climate-relevant processes, such as new particle formation, particularly in remote regions. Here, we present highly sensitive, online observations of gaseous ammonia from a coastal site in Antarctica, which allows us to constrain the mechanism of new particle formation in this region in unprecedented detail. Our observations show that penguin colonies are a large source of ammonia in coastal Antarctica, whereas ammonia originating from the Southern Ocean is, in comparison, negligible. In conjunction with sulfur compounds sourced from oceanic microbiology, ammonia initiates new particle formation and is an important source of cloud condensation nuclei. Dimethylamine, likely originating from penguin guano, also participates in the initial steps of particle formation, effectively boosting particle formation rates up to 10000 times. These findings emphasize the importance of ecosystem processes from penguin/bird colonies and oceanic phytoplankton/bacteria on climate-relevant aerosol processes in coastal Antarctica. This demonstrates an important connection between ecosystem and atmospheric processes that impact the Antarctic climate, which is crucial given the current rate of environmental changes in the region.

Biological processes influence atmospheric composition and climate through a variety of mechanisms. For example, living organisms emit vapors that moderate cloud properties via the production of aerosol and cloud condensation nuclei (CCN) or ice nucleating particles (INP), which subsequently impact Earth's surface radiative balance, precipitation, and weather. Changes in the biology of an ecosystem can therefore impact climate.

Vegetation in continental regions emits volatile organic vapors, which are subsequently converted to secondary organic aerosol¹. In pristine marine

and polar environments, however, aerosol and CCN production is connected to marine phytoplankton dimethyl sulfide (DMS) and iodine emissions via new particle formation (NPF)².

In the remote Southern Ocean and Antarctica, the strength of NPF events has considerable relevance for the climate. These pristine locations typically have low background particle concentrations compared to regions with anthropogenic activities or vegetation. Coincidentally, the chemical mechanism of NPF remains elusive in remote and polar regions, yet NPF is estimated to contribute over 50% of CCN in the atmosphere globally³, and

¹Institute for Atmospheric and Earth System Research (INAR)/Physics, University of Helsinki, Helsinki, Finland. ²Aerodyne Research Inc., 45 Manning Road, Billerica, MA, USA. ³Palas GmbH, Karlsruhe, Germany. ⁴Servicio Meteorológico Nacional, Av. Dorrego 4019, CABA, Argentina. ⁵Department of Applied Physics, University of Eastern Finland, Kuopio, Finland. ⁶Department of Physics, Lund University, Professorsgatan 1, Lund, Sweden. ⁷Departamento de Biología de Predadores Tope, Programa Monitoreo del Ecosistema, Instituto Antártico Argentino, 25 de Mayo 1143, B1650CSP San Martín, Buenos Aires, Argentina. ⁸Yusuf Hamied Department of Chemistry, University of Cambridge, Cambridge, UK. ⁹Faculty of Biological and Environmental Sciences, University of Helsinki, Helsinki, Finland. ¹⁰Atmospheric Composition Research, Finnish Meteorological Institute, Helsinki, Finland. ✉e-mail: matthew.boyer@helsinki.fi; mikko.sipila@helsinki.fi

potentially more in such environments, including over the Antarctic continent⁴. Interactions of aerosols and clouds, especially the sources and concentrations of CCN in pristine, preindustrial-like environments, are a large source of uncertainty in our understanding of climate change⁵. Climate-relevant cloud properties, such as cloud brightness and lifetime, are very sensitive to the concentration of CCN in such conditions⁶. Therefore, the gases that contribute to NPF events, and their ability to enhance particle formation rates, are critical to understanding the climate response in these locations.

Direct observations of DMS-derived sulfuric acid (H_2SO_4) aerosol formation in the polar regions indicate that ammonia (NH_3) stabilizes sulfuric acid clusters during NPF events^{2,7,8}. Seabirds are a known source of atmospheric ammonia in remote regions^{9–12}, and studies present evidence that ammonia emissions from penguins/seabirds impact aerosol formation and cloud processes^{2,7,8,13,14}. Even though laboratory experiments have shown that ammonia can enhance sulfuric acid-induced particle formation by several orders of magnitude¹⁵, there are few measurements of ammonia concentrations in the remote ambient atmosphere with high enough sensitivity and time resolution coupled with comprehensive measurements to resolve the mechanism of NPF.

Iodic acid (HIO_3) has been shown to contribute to NPF together with iodic acid (HIO_2)^{16–18} in the absence of sulfuric acid and ammonia in sea ice-covered regions in the Arctic during spring and autumn. While these particles may contribute to CCN¹⁷, other observations suggest that they rarely grow to climate-relevant CCN sizes². A recent laboratory study has also proposed that NPF may occur between iodine oxoacids and sulfuric acid without ammonia in remote marine and polar environments, and the presence of approximately 30–260 ppt of ammonia can further enhance aerosol nucleation rates¹⁹. Their conclusions assume that there is at maximum a few hundred ppt of ammonia in the remote polar atmosphere to participate, based on limited ambient data from these environments. Similarly, another study suggested that sulfuric acid and amines, sourced from sea-ice-covered regions, dominate particle formation around the Antarctic Peninsula²⁰. Alkylamines, such as dimethylamine (DMA, $(\text{CH}_3)_2\text{NH}_2$), are known to nucleate rapidly with sulfuric acid^{21,22}, yielding formation rates up to 10000 times faster than sulfuric acid-ammonia NPF. These discrepancies show that the chemical mechanism of NPF in this environment remains poorly constrained, where direct measurement of ammonia and amine concentrations comprises a key knowledge gap.

In general, ammonia is one of the most under-represented gases in atmospheric measurements, especially online measurements at high sensitivity and in remote regions where ambient ammonia concentrations are estimated to be low (i.e., lower than 100 ppt). However, without ammonia measurements, we are missing critical observations that limit our understanding of climate-relevant aerosol formation processes. The lack of data is particularly pronounced in our ability to constrain new particle formation (NPF) in remote and polar environments.

Currently, Antarctic ecosystems are stressed. The region is experiencing accelerated changes due to warming. Within the past decade, sea ice extent has started declining²³, and ice shelves are shrinking²⁴. These changes impact the biology in the Southern Ocean²⁵, as well as penguin and seabird colonies, which will result in changes to ecosystem-atmosphere exchanges, and ultimately the climate of the region, with subsequent effects on global climate. Some species of penguins are already threatened due to environmental changes²⁶. Therefore, it is imperative to understand the ecosystem-atmosphere interactions that contribute to climate-relevant processes, especially now, as environmental conditions in coastal Antarctica and the Southern Ocean are rapidly changing.

In this work, we analyze the chemical mechanism of NPF events on the Antarctic Peninsula, featuring highly sensitive online measurements of ambient ammonia concentrations as well as comprehensive measurements of gases and particles to investigate aerosol processes connecting NPF with cloud formation. We show that penguins are a large source of ammonia that enhances NPF with sulfuric acid sourced from marine phytoplankton in coastal Antarctica, whereas ammonia contributions from the open ocean

were negligible. We present evidence that these newly formed particles can grow and contribute to CCN concentrations and cloud/fog formation. This demonstrates that penguins/sea birds play a key role in particle formation and may represent an important climate feedback as their habitat changes.

Results

Our study combines measurements of aerosol precursor vapors concentrations, ammonia mixing ratios, the chemistry of charged nucleating clusters, aerosol particle number concentrations and size distributions, aerosol chemical composition, CCN concentrations, and in situ cloud droplet distributions from Marambio station on the Antarctic peninsula (Fig. 1A, B) to investigate the connection between gases, particles, and clouds. In our measurements, we observed ammonia mixing ratios up to 13.5 ppb when winds came from the direction of nearby penguin colonies, as shown in Fig. 1 and Supplementary Fig. 1. In contrast, from other wind directions (including the open ocean), ammonia mixing ratios were low. Excluding the influence of local pollution from Marambio station (19.4% occurrence), 42.8% of the measured ammonia mixing ratios were below the detection limit (10.5 ± 26.8 ppt), 36.2% were between 10.5 and 40 ppt, 9.8% were between 40 and 100 ppt, and 11.2% were greater than 100 ppt (Fig. 1D).

Notably, the penguins in the nearby colony left their breeding site in the middle of our measurement campaign as part of their annual migration. For over a month after the penguins left, concentrations of ammonia remained elevated, exceeding 1 ppb (Supplementary Fig. 2) from the favorable wind direction. Therefore, the penguin guano “fertilized” soil, also known as ornithogenic soil²⁷, continued to be a strong source of ammonia long after they left the site. Until now, this process has largely only been evaluated in laboratory measurements²⁸, models^{10,12,29}, or offline methods³⁰. Our data demonstrates that there are local hotspots around the coast of Antarctica that can yield ammonia concentrations similar in magnitude to agricultural plots^{31,32} during summer. These hotspots correspond to the location of penguin/bird breeding settlements/colonies, consistent with previous studies. Due to the spatial distribution of penguin/seabird colonies, these hotspots may cover a large extent of coastal Antarctica^{33,34}.

Our results demonstrate that ammonia is present in the Antarctic environment at sufficient mixing ratios to initiate NPF with sulfuric acid. In fact, we observed NPF almost exclusively when winds were from the direction/wind sector of local penguin colonies, leading to elevated ammonia mixing ratios. Particle formation rates ($J_{1.7}$) during these NPF events depended primarily on sulfuric acid concentrations, however, our observations of aerosol precursor vapors, the chemical composition of atmospheric clusters, and online measurement of ammonia show clear participation of ammonia and enhancement of particle formation rates when ammonia mixing ratios exceed ~100 ppt (Fig. 2). We did not uniformly observe continued enhancement as ammonia mixing ratios increase above ~100 ppt, indicating that particle formation with respect to ammonia begins to saturate at this level, similar to laboratory-derived estimates of ammonia saturation in sulfuric acid-ammonia clustering studies^{15,35}.

Additionally, we compared our observations to a formation rate parameterization that considers sulfuric acid and ammonia concentrations³⁶. The measured formation rates are consistently between 1 and 4 orders of magnitude higher than the parameterization (median ratio = 72). It is important to note that there are several possible reasons for discrepancies, particularly with respect to field observations, including errors inherent in the measurements and calculation of formation rates and a factor of two uncertainty in the calibration and quantification of sulfuric acid concentrations. Despite these uncertainties, we can attribute the higher formation rates in our observations to the participation of other gases that can further enhance particle formation rates of the sulfuric acid-ammonia mechanism.

While the chemical composition of charged clusters during NPF is dominated by sulfuric acid and ammonia clusters (Fig. 3A), there are additional clusters present, indicating a multicomponent particle formation mechanism. These include sulfuric acid and DMA clusters, which are known to yield particle formation rates between 100 and 10000 times

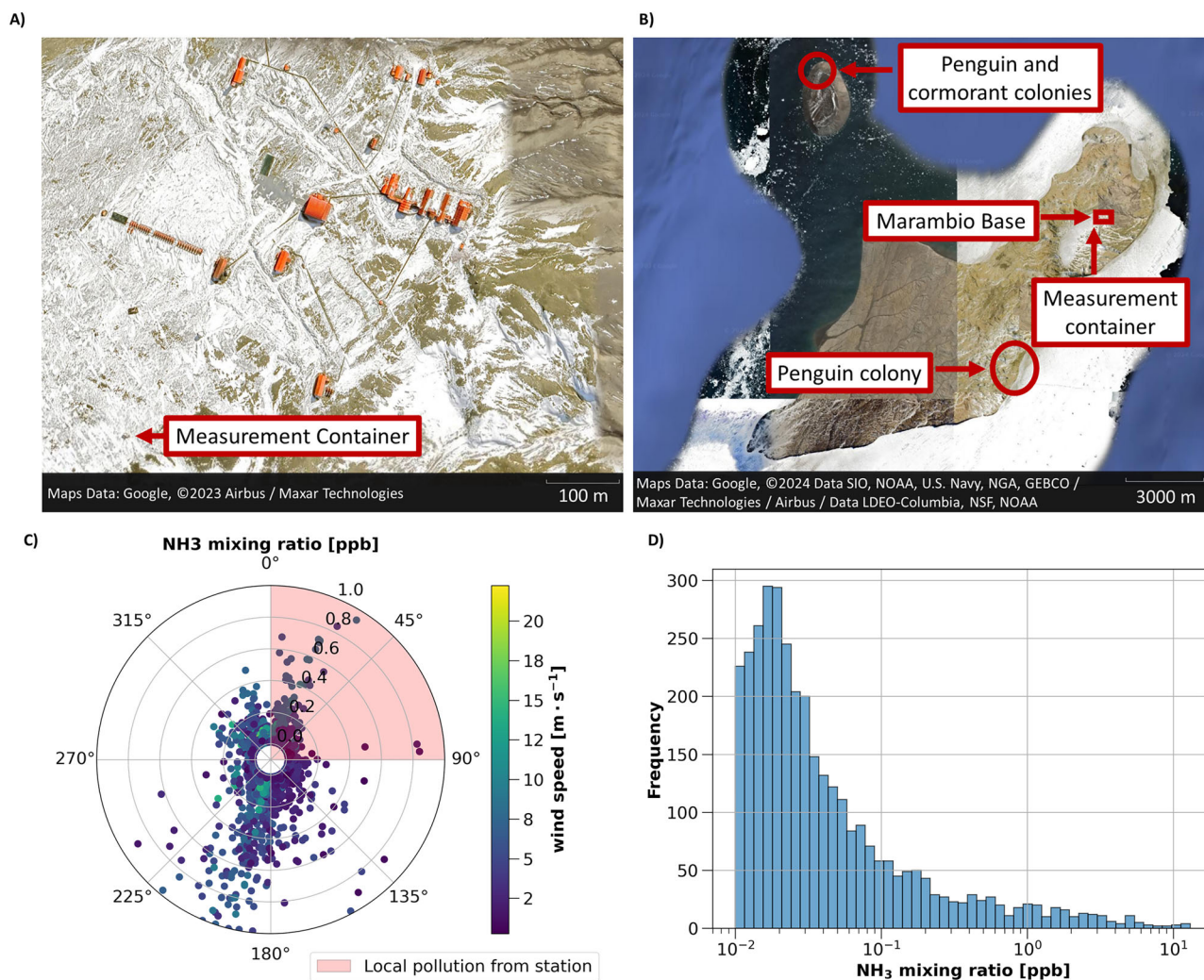


Fig. 1 | Sources of ammonia at Marambio Station, Antarctica. **A** A map showing the location of the measurement container with respect to the buildings and facilities of Marambio Station. **B** A map showing the relevant points of interest for ammonia on Seymour Island. **C** A wind rose showing the ammonia mixing ratios between 0.01

and 1 ppb according to wind direction and wind speed. Note that the mixing ratio axis is zoomed to a maximum of 1 ppb to show further details in the lower range of mixing ratios. **D** The frequency of observed NH_3 mixing ratios.

faster than sulfuric acid and ammonia²². Previously, DMA-containing clusters were observed to dominate at DMA mixing ratios of 4 ppt in the presence of ammonia exceeding 1 ppb³⁷. Here, instead, sulfuric acid and ammonia clusters are the dominant growing clusters, suggesting that DMA is present at very low concentrations—enough to stabilize the initial stages of cluster formation and enhance sulfuric acid-ammonia particle formation rates by $\sim 2\text{--}4$ orders of magnitude compared to pure sulfuric acid-ammonia nucleation (Fig. 3C). These conclusions agree with the findings of Quéléver et al.⁸

It is worth noting that we cannot determine the gas phase DMA concentration from cluster measurements, but the detection of DMA in atmospheric clusters in the API-ToF, which is believed to be the most sensitive detector for the presence of atmospheric amines, does confirm the presence of DMA²². We can use the ion counts of clusters containing DMA (in counts per second) to estimate changes in available DMA (Fig. 3B), but this is qualitative; a direct measure of DMA should be prioritized in future measurements. Despite this limitation on the quantification of DMA, we conclude that DMA does indeed play a role in enhancing formation rates. By comparing with previous chamber measurements²², we can estimate the DMA mixing ratios in our measurements (Fig. 3D). It is important to note that the formation rates reported from the chamber experiments²² are at times underestimated³⁸, hence we estimate that DMA mixing ratios are

likely <1 ppt. Although we cannot offer strong comments on the concentrations or sources of DMA without direct measurements, wind rose directions with the highest ion counts of DMA in clusters are similar to those associated with high ammonia mixing ratios (Supplementary Fig. 1). Penguin guano has also been identified to produce amines in guano-affected soils³⁹. Therefore, it is plausible that penguin colonies, in addition to sea-ice-covered regions⁴⁰, are a source of DMA and other alkylamines.

Recent observations suggest that clustering between sulfuric acid and DMA is the primary mechanism of particle formation around coastal Antarctica, where DMA is sourced from sea-ice-covered regions²⁰. Interestingly, Brean et al.²⁰ did not observe sulfuric acid-ammonia clusters in their measurements. In contrast, our observations show ammonia-dominated clustering with sulfuric acid instead of amine-mediated cluster growth. In comparison to Brean et al.²⁰, NPF occurred more frequently during our study and produced higher concentrations of new particles. We observed NPF on 34% of our measurement days, resulting in enhanced aerosol concentrations at times exceeding $15,000 \text{ \#}/\text{cm}^3$, as shown in Fig. 4C. Therefore, we propose that while amines, originating from sympagic and pelagic sources^{40–42}, may enhance NPF in parts of the Southern Ocean or coastal Antarctica the multicomponent formation mechanism with sulfuric acid, DMA, and ammonia has a stronger impact on particle concentrations, and subsequently the climate-relevant aerosol formation in these regions.

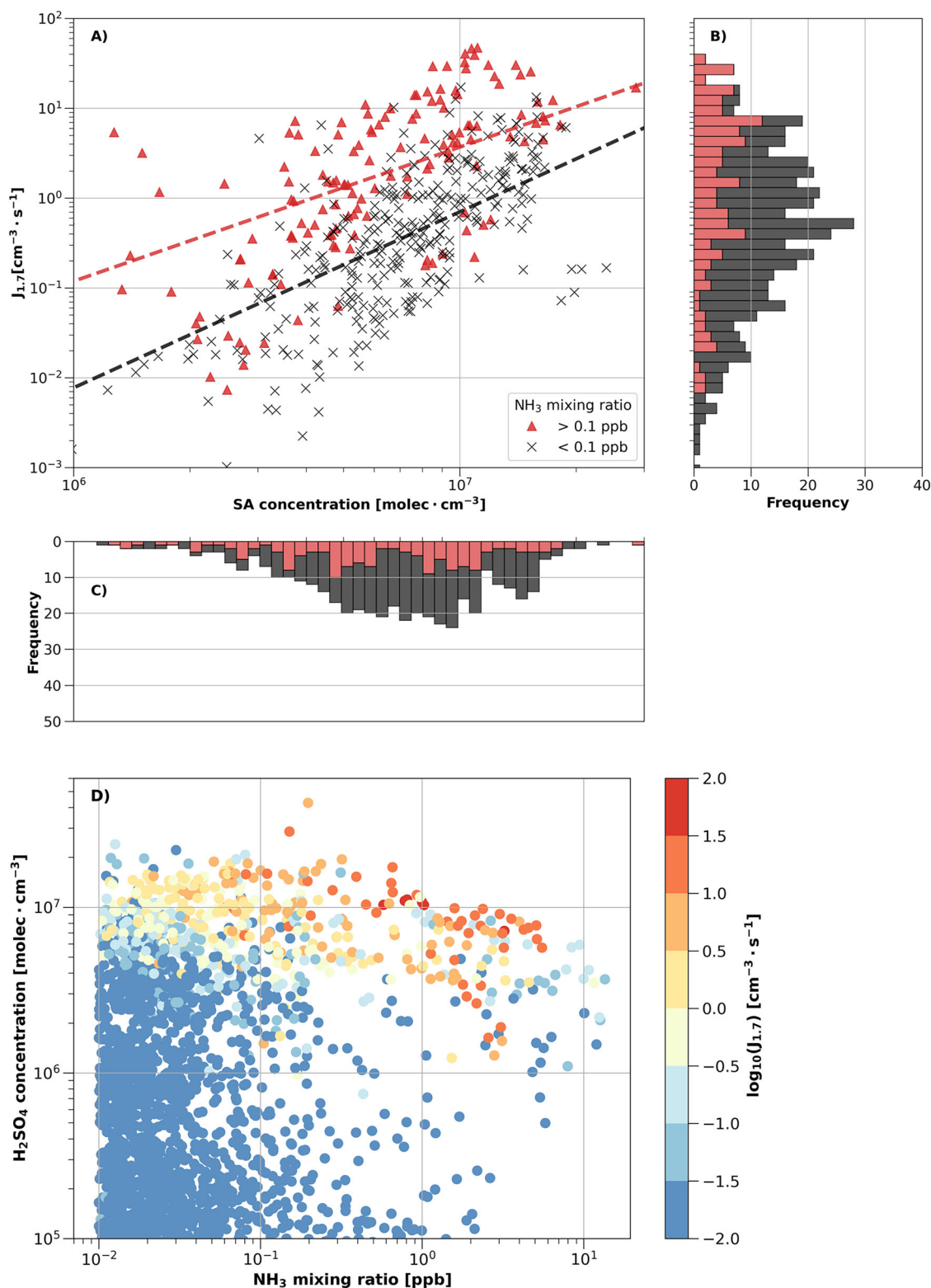


Fig. 2 | Ammonia saturation and enhancement in particle formation rates.

A Measured negative ion formation rates, $J_{1.7}$, are presented against sulfuric acid concentration during NPF events. Ammonia mixing ratios above and below 0.1 ppb are shown with red triangles and black crosses, respectively, and the red and black dashed lines are drawn to guide the eyes for these two groups. **B** The frequency of observed particle formation rates during NPF events, where the corresponding

ammonia mixing ratios above and below 0.1 ppb are shown by the red (above) and black (below) bars. **C** The frequency distribution of SA concentrations with the range of ammonia mixing ratios is shown by the red and black bars. **D** A scatter plot of SA and ammonia measurements during the campaign, where the color bar represents the calculated formation rate of negative ions at 1.7 nm ($J_{1.7}$).

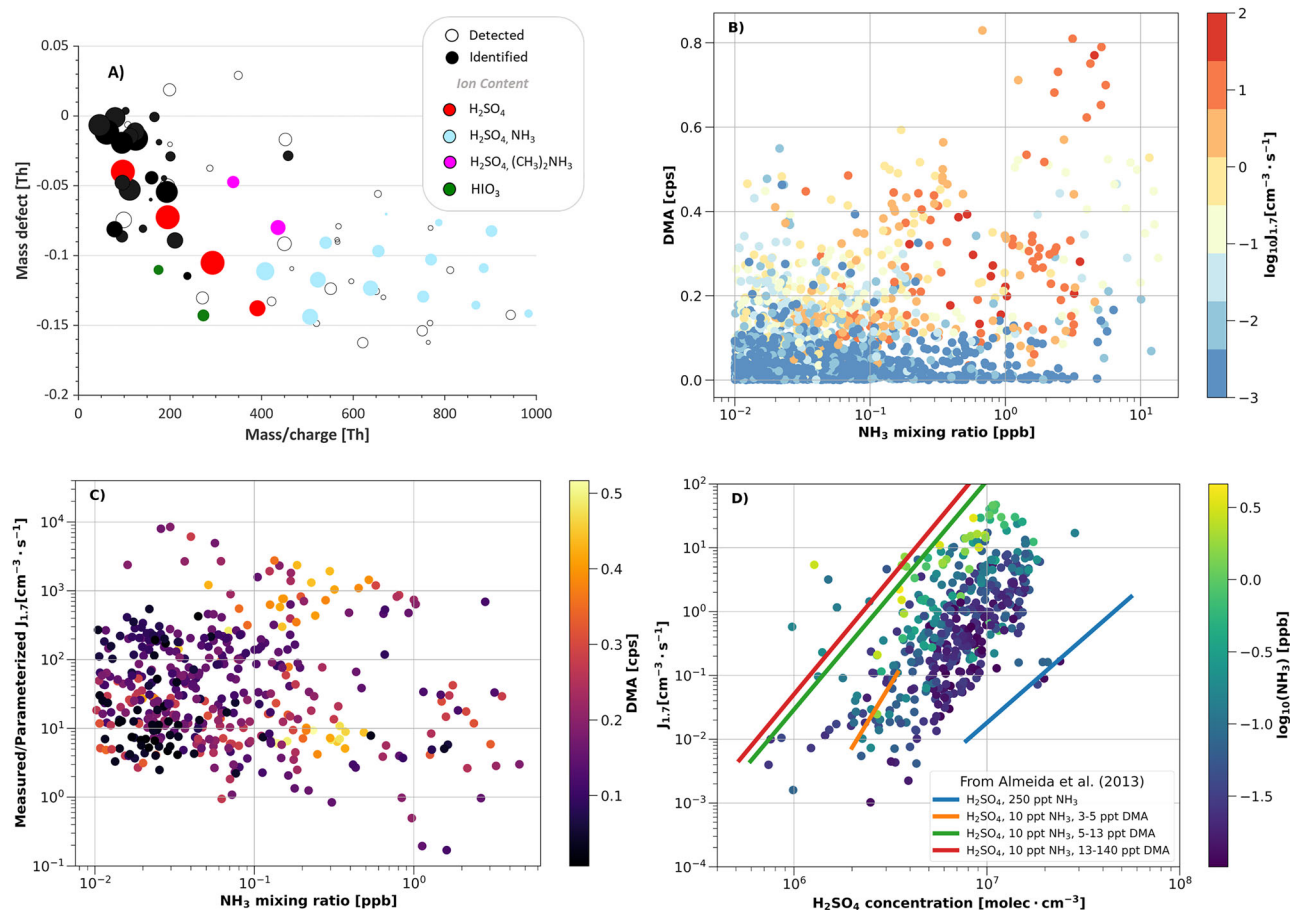


Fig. 3 | The multicomponent mechanism of NPF. **A** A representative mass defect plot showing the chemical composition of the negatively charged clusters during NPF. The colored circles indicate clusters of known composition, where the size corresponds to their relative signal magnitude in counts per second. The data shown are the average signal intensities measured over an NPF event. **B** Ammonia mixing ratios and the signal intensity of DMA. The color bar shows the measured particle formation rates during the campaign. **C** A comparison of the measured particle formation rates, $J_{1,7}$, compared to formation rates predicted using the Dunne et al.³⁶ parameterization of the sulfuric acid-ammonia nucleation mechanism. The comparison is presented as the ratio of measured/parameterized formation rates against

ammonia mixing ratios, where the color bar indicates the signal intensity of DMA in counts per second. The presented data only includes periods identified as NPF events. **D** A comparison between our measurements and CLOUD chamber experiment observations of the nucleation mechanism with DMA, ammonia, and sulfuric acid. The colored lines represent the expected particle formation rates at various concentrations of sulfuric acid, DMA, and ammonia from Almeida et al.²², and the points show the measured formation rates compared according to sulfuric acid concentrations. The color bar indicates the corresponding ammonia mixing ratios.

Observations of the atmospheric cluster composition also show participation of iodine oxoacids (HIO_2 and HIO_3) in some cases (Supplementary Fig. 3). Although it should be noted that ammonia and amines had a more pronounced role in particle formation in our measurements, as the sulfuric acid-ammonia clusters dominated ionic cluster chemistry, the multicomponent system with ammonia, sulfur, and iodine compounds is a valuable finding. It is important to consider that our measurements only cover the summer period when conditions favor the strongest photochemical production of sulfur compounds from DMS and when penguin breeding colonies are present, whereas the production of iodine oxoacids is expected to be stronger during seasonal transitions in spring and fall^{17,43}. During seasonal transitions, particle formation may show stronger enhancement from iodine oxoacids; however, in situ observations of the chemical mechanism of NPF during seasonal transitions in Antarctica are lacking, and therefore, it calls for future dedicated studies.

NPF in Antarctica has been observed to contribute to background CCN concentrations⁴⁴. Our measurements also demonstrate the connection between NPF, CCN formation, and fog/cloud droplet activation. From a case study on February 1, 2023, we had a very strong NPF and growth event with ammonia from the penguin colonies, resulting in very high concentrations of particles ($>16,000 \# \cdot \text{cm}^{-3}$ above 10 nm), as shown in Fig. 4.

These particles grew over the next 6 h up to ~ 30 nm, followed by a period of fog. While sampling in the fog, we measured a reduction in nucleation mode particles from scavenging and an increase in larger particles from cloud droplet residuals, which likely result from rapid growth of particles due to cloud processing⁴⁵. Activated particles are present at all supersaturations in the CCN counter measurements, and the particle composition was dominated by ammonium sulfate. After the 1-hour period in fog, the fog lifted such that sampling occurred below the fog/cloud layer, after which the same mode of newly formed particles was observed again. The persistence in the newly formed particle mode before and after the fog signifies strong regional NPF during which these particles influenced fog microphysics by contributing to the fog/cloud droplet population. The chemical composition of the cloud droplet residuals was composed almost solely of ammonia sulfate, which confirms the participation of ammonia sourced from the penguins. Further details of this case study are discussed in Supplementary Note 1.

Broader climate implications

Recent observations suggest that aerosol precursor gases in Antarctica are closely linked to regional ecosystem processes^{7,8,20,41,42}. Key sulfur compounds originate from DMS emissions due to marine phytoplankton in the Southern Ocean around coastal Antarctica, which has one of the highest

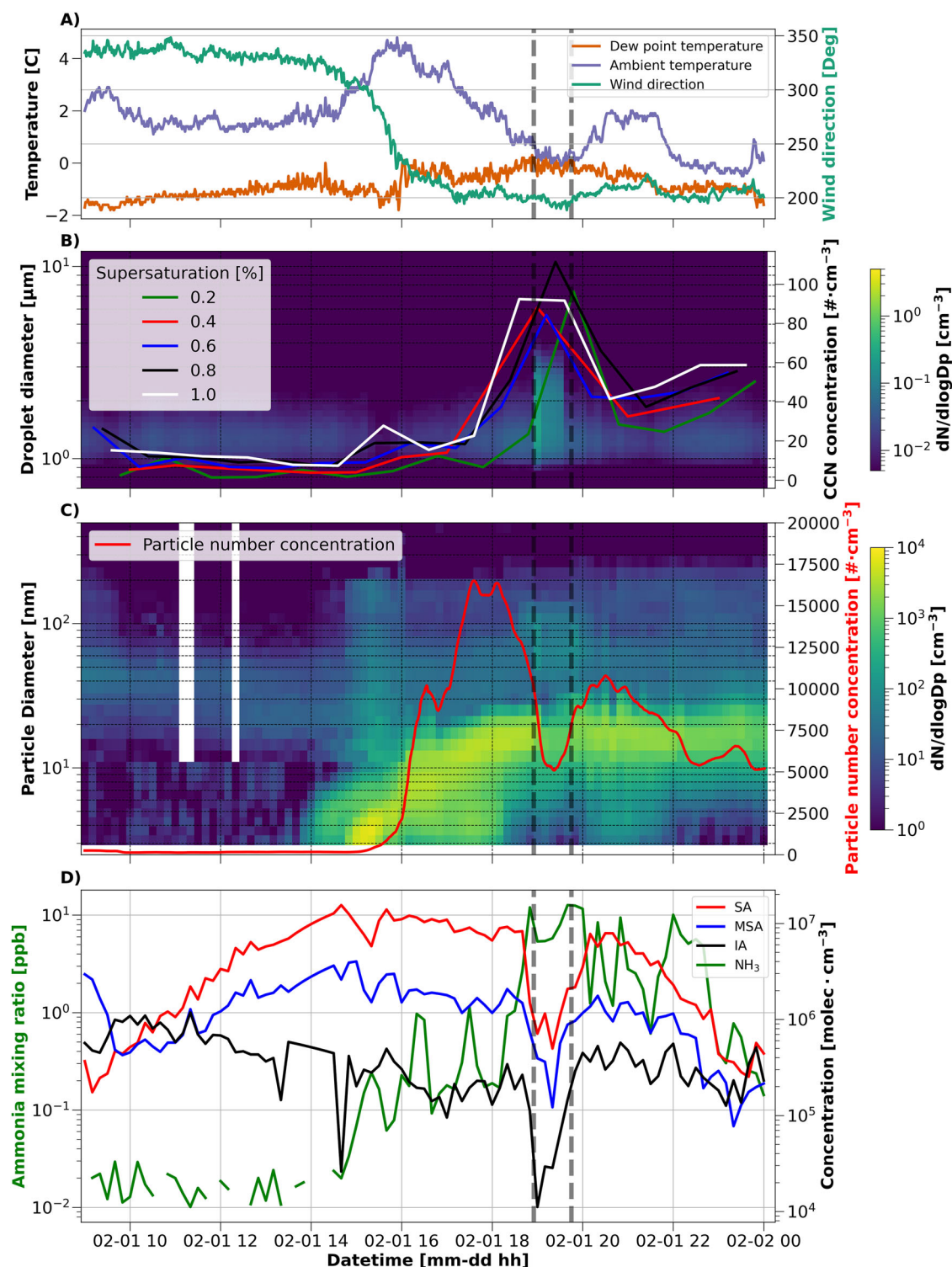


Fig. 4 | Case study: the connection between NPF, CCN, and clouds in our measurements. The timeseries of various atmospheric measurements from a case study on February 01, 2023, during which regional particle formation, growth, and subsequent cloud formation were observed. The dashed gray lines indicate the period while sampling in fog. **A** Relevant meteorological condition, including ambient temperature (purple line), dew point temperature (orange line), and wind direction (green line), during the case study. **B** The number size distribution of particles/

droplets > 0.7 microns and CCN concentrations from 5 different supersaturations (0.2%: green line, 0.4%: red line, 0.6%: blue line, 0.8%: black line, 1.0%: white line). **C** The particle number size distribution > 3 nm and the particle number concentrations (red line). **D** The mixing ratio of ammonia (NH_3 ; green line), and the concentrations of sulfuric acid (SA; red line), methanesulfonic acid (MSA; blue line), and iodic acid (IA; black line).

DMS concentrations on the planet during summer^{46,47}. Iodine compounds are also sourced from processes involving ocean biology and heterogeneous chemistry on ice and snow surfaces⁴³. Now, we quantify the contribution of ammonia from penguins/sea birds at mixing ratios high enough to initiate

and enhance NPF with sulfuric acid from DMS. Our measurements demonstrate that penguin colonies form strong point sources of particles in a region where cloud formation can be limited by the availability of CCN. In general, the radiative properties of clouds are sensitive to the number of

CCN; hence, the strength of NPF impacts climate-relevant cloud processes. Given that penguin colonies span the coast of Antarctica³³ and that they leave guano/nutrient-rich soils that continue to emit ammonia after migration, we estimate that penguins provide a substantial source of ammonia that enhances particle concentrations across the entire coastal Antarctic region^{12,34}.

While the lifetime of gaseous ammonia in the troposphere is estimated to be short, ranging from several hours to ~1 day^{32,48}, the lifetime of the particles that result from NPF events has longer lifetimes up to several days⁴⁹. These newly formed particles could be further transported over parts of the Southern Ocean and continental Antarctica on this timescale, which could subsequently affect aerosol and CCN concentrations over the larger Antarctic region, including further inland⁷ where aerosol sources are limited⁵⁰. This suggests that coastal penguin/bird colonies could also comprise an important source of aerosol away from the coast.

It is already understood that widespread loss of sea ice extent threatens the habitat, food sources⁵¹, and breeding behavior⁵² of most penguin species that inhabit Antarctica. Consequently, some Antarctic penguin populations are already declining²⁶, and some species could be nearly extinct by the end of the 21st century⁵³. We provide evidence that declining penguin populations could cause a positive climate warming feedback in the summertime Antarctic atmosphere, as proposed by a modeling study of seabird emissions in the Arctic region¹⁴.

Furthermore, our results demonstrate a multicomponent nucleation mechanism between sulfuric acid and ammonia over broad concentration ranges of both these precursors in ambient conditions and in the absence of anthropogenic influence or vegetation. NPF events rarely occur in the remote marine boundary layer, including over the Southern Ocean, despite the presence of condensable vapors from DMS oxidation⁵⁴. Studies in other environments also suggest that NPF in the ambient atmosphere occurs more readily when ammonia is available^{55–57}, or that ammonia enhances NPF⁵⁸. We show that ammonia from penguins stabilizes sulfuric acid clusters from DMS oxidation over Antarctica and, together with low-level DMA, yields high particle formation rates that can grow to CCN-active particles. We also identify that the Southern Ocean is not a noteworthy source of gaseous ammonia, at least in its current state⁵⁹, which offers a possible explanation for the limited observations of NPF events in the remote marine boundary layer. Therefore, we demonstrate that the ammonia budget is critical to understanding the contribution of DMS to NPF in coastal Antarctica, which may also have global atmospheric implications, including in the past, present, and future. The potential contribution of iodine oxoacids may also be important in this context, as they may serve as the “base” to initiate sulfuric acid nucleation at low ammonia concentrations during seasonal transitions. Fundamentally, the prevalence of these gases over Antarctica depends upon the interplay of sea ice, phytoplankton metabolism, and penguin/sea bird populations—all of which are subject to change. The complexity of these processes requires continued, dedicated experimentation and investigation to deconvolve.

Methods

Measurement site

All measurements reported in this work were collected during austral summer between January 10 and March 20, 2023, in the atmospheric observatory located ~300 m southwest of Marambio Station, Antarctica (64°14.68' S, 56°37.88' W; Fig. 1A, B) at an altitude of 198 m above sea level. Marambio station is located on Seymour Island near the northernmost tip of the Antarctic Peninsula. Further descriptions of the measurement site, including the typical meteorological conditions and aerosol observations, are given in Asmi et al.⁶⁰ and Quéléver et al.⁸.

Various features of the measurement site near Marambio station are important for the interpretation of our measurements. Logistical activities at the station contributed a local source of pollution that contaminated the ambient sampling when wind directions originated from between 0° and 90° and were excluded from our analysis. Measurements of particle number concentrations, black carbon, and carbon monoxide from the measurement

container were also used to confirm the presence of pollution in the dataset. A large colony of Adelie penguins (*Pygoscelis adeliae*) with approximately 30,000 breeding pairs⁶¹ was located ~8 km southwest (~200°) of the measurement station. Penguins were present at the colony for the first half of the campaign, until February 21, 2023 (Pablo J. Perchivale, personal observations), when the last birds departed the breeding site for their wintering grounds. A second colony of Adelie penguins was located on Cockburn Island, ~10 km northwest (~330 degrees) of the measurement site. Although the Cockburn Island colony has fewer breeding pairs, about 15,721⁶², than the colony located to the south, this colony shares the breeding area with a colony of imperial shags (*Phalacrocorax bransfieldensis*) with approximately 800 breeding pairs⁶³. The direction of these penguin/seabird colonies also corresponds with the prevailing wind directions at the measurement site, as presented in Asmi et al.⁶⁰.

Instrumentation

Ammonia mixing ratios were measured using a Quantum Cascade Tunable Infrared Laser Differential Absorption Spectrometer^{64,65} (QC-TILDAS, Aerodyne Research, Inc.). Refer to Supplementary Note 2 for further details of the ammonia QC-TILDAS.

Aerosol precursor vapors and cluster chemistry were measured using a chemical ionization mass spectrometer⁶⁶ (CIMS, ToFwerk) with a multi-scheme chemical ionization inlet⁶⁷ (MION, Karsa Ltd.). The MION inlet was used to cycle between two measurement modes: chemical ionization with NO₃[−] ion and ambient ions. The NO₃[−] mode was used to measure the concentrations of the neutral condensable vapor species, including sulfuric acid, methanesulfonic acid, and iodic acid. A dedicated sulfuric acid calibration, following the procedure outlined in Kürten et al.⁶⁸, was performed before and after the campaign to enable concentration retrieval from the NO₃[−] mode. There is an accuracy of 33% associated with the calibration factor using this method⁶⁸, and the uncertainty in the reported concentrations obtained from NO₃[−]-CIMS is estimated to be −50% to +100%⁶⁶. The ambient ion mode was used to determine the chemical composition of the growing clusters during NPF events.

The size distribution of atmospheric ions from 0.75 to 40 nm was measured using a neutral air ion spectrometer^{69,70} (NAIS, Airel). Particle number size distributions from 10 to 800 nm were provided by a differential mobility particle spectrometer (DMPS)⁷¹. The DMPS system used a Hauke-type differential mobility analyzer⁷². A merged size distribution product combining the NAIS and DMPS distributions was used in the relevant calculations of aerosol parameters, where the particle concentrations in the NAIS were scaled down by a factor of 3 to account for overcounting in the particle modes in our data⁵⁸.

CCN concentrations were measured using a CCN counter⁷³ (CCN-100, Droplet Measurement Technologies) with scans at five supersaturation setpoints (0.2, 0.4, 0.6, 0.8, and 1.0%). The CCN counter sampled downstream of the differential mobility analyzer in the DMPS system to obtain scans of size-resolved CCN concentrations.

Aerosol chemistry was measured using a Time-of-Flight Aerosol Chemical Speciation Monitor⁷⁴ (ToF-ACSM, Aerodyne Research, Inc.).

In-situ cloud droplet number concentrations and size distributions between 0.2 and 40 μm were measured using a cloud droplet analyzer (CDA, Palas GmbH), located on the roof of the measurement container. The optical sensor in the CDA has been previously described in the literature⁷⁵.

An automatic weather station, installed on the measurement container, measured global radiation (pyranometer, CMP11, Kipp & Zonen), ambient temperature and relative humidity (HMP155, Vaisala Ltd.), and wind speed and direction (ultrasonic anemometer, Thies 2D, Thies Clima), as described in Quéléver et al.⁸.

Calculations of aerosol parameters

Particle growth rates between 3 and 7 nm were calculated from the NAIS size distributions using both the maximum-concentration method and log-normal distribution function method presented in Kulmala et al.⁷⁶. The median growth rate was used in the formation rate calculation.

Formation rates of atmospheric ions at 1.7 nm ($J_{1.7}$) were calculated using the number size distributions of negative ions from the NAIS according to Eq. (10) in Kulmala et al.⁷⁶ using a particle bin of 1.7–3.1 nm:

$$J_{d_p} = \frac{dN_{d_p}^-}{dt} + \text{CoagS}_{d_p} \cdot N_{d_p}^- + \frac{GR}{\Delta d_p} \cdot N_{d_p}^- + \alpha \cdot N_{d_p}^- \cdot N_{<d_p}^- - \chi \cdot N_{d_p} \cdot N_{<d_p}^-, \quad (1)$$

where J^- is the formation rate, N^- is the measured concentration of negative ions, t is time, CoagS is the coagulation sink, GR is the particle growth rate between 3 and 7 nm, Δd_p is the difference in diameters in the selected range of particle bins, α is the ion–ion recombination coefficient, χ is the ion–aerosol attachment coefficient, and N is the measured concentration of neutral particles. The subscript d_p refers to the diameter associated with this formation rate, which is 1.7 nm in this study, and the subscript $<d_p$ refers to all diameters smaller than d_p . The coagulation sink and condensation sink were determined using Eqs. (4) and (5) in Kulmala et al.⁷⁶, respectively, and $1.6 \cdot 10^{-6} \text{ cm}^3 \text{ s}^{-1}$ and $0.01 \cdot 10^{-6} \text{ cm}^3 \text{ s}^{-1}$ are typical values of α and χ , respectively. Given uncertainties inherent to the measurement of sub 3 nm particles associated the NAIS, we estimate a factor of 2–5 uncertainty in the reported formation rates⁷⁷. A comprehensive overview of the uncertainties associated with measurements sub 3 nm particles/ions is in given in Kangasluoma et al.⁷⁸.

Data availability

The datasets used for this study are publicly available at <https://doi.org/10.5281/zenodo.15210312>.

Received: 19 November 2024; Accepted: 17 April 2025;

Published online: 22 May 2025

References

- Ehn, M. et al. A large source of low-volatility secondary organic aerosol. *Nature* **506**, 476–479 (2014).
- Beck, L. J. et al. Differing mechanisms of new particle formation at two arctic sites. *Geophys. Res. Lett.* **48**, e2020GL09133 (2021).
- Merikanto, J., Spracklen, D. V., Mann, G. W., Pickering, S. J. & Carslaw, K. S. Atmospheric chemistry and physics impact of nucleation on global CCN. *Atmos. Chem. Phys.* **9**, 8601–8616 (2009).
- Gordon, H. et al. Causes and importance of new particle formation in the present-day and preindustrial atmospheres. *J. Geophys. Res. Atmos.* **122**, 8739–8760 (2017).
- Carslaw, K. S. et al. Large contribution of natural aerosols to uncertainty in indirect forcing. *Nature* **503**, 67–71 (2013).
- Mauritsen, T. et al. An Arctic CCN-limited cloud-aerosol regime. *Atmos. Chem. Phys.* **11**, 165–173 (2011).
- Jokinen, T. et al. Ion-induced sulfuric acid-ammonia nucleation drives particle formation in coastal Antarctica. *Sci. Adv.* **4**, eaat9744 (2018).
- Quéléver, L. L. J. et al. Investigation of new particle formation mechanisms and aerosol processes at Marambio Station, Antarctic Peninsula. *Atmos. Chem. Phys.* **22**, 8417–8437 (2022).
- Schmale, J. et al. Sub-Antarctic marine aerosol: dominant contributions from biogenic sources. *Atmos. Chem. Phys.* **13**, 8669–8694 (2013).
- Riddick, S. N. et al. High temporal resolution modelling of environmentally-dependent seabird ammonia emissions: Description and testing of the GUANO model. *Atmos. Environ.* **161**, 48–60 (2017).
- Wentworth, G. R. et al. Ammonia in the summertime Arctic marine boundary layer: sources, sinks, and implications. *Atmos. Chem. Phys.* **16**, 1937–1953 (2016).
- Riddick, S. N. et al. The global distribution of ammonia emissions from seabird colonies. *Atmos. Environ.* **55**, 319–327 (2012).
- Weber, R. J. et al. A study of new particle formation and growth involving biogenic and trace gas species measured during ACE 1. *J. Geophys. Res. Atmos.* **103**, 16385–16396 (1998).
- Croft, B. et al. Contribution of Arctic seabird-colony ammonia to atmospheric particles and cloud-albedo radiative effect. *Nat. Commun.* **7**, 13444 (2016).
- Kirkby, J. et al. Role of sulphuric acid, ammonia and galactic cosmic rays in atmospheric aerosol nucleation. *Nature* **476**, 429–433 (2011).
- Sipilä, M. et al. Molecular-scale evidence of aerosol particle formation via sequential addition of HIO₃. *Nature* **537**, 532–534 (2016).
- Baccarini, A. et al. Frequent new particle formation over the high Arctic pack ice by enhanced iodine emissions. *Nat. Commun.* **11**, 4924 (2020).
- He, X.-C. et al. Role of iodine oxoacids in atmospheric aerosol nucleation. *Science* **371**, 589–595 (2021).
- He, X.-C. et al. Iodine oxoacids enhance nucleation of sulfuric acid particles in the atmosphere. *Science* **382**, 1308–1314 (2023).
- Brean, J. et al. Open ocean and coastal new particle formation from sulfuric acid and amines around the Antarctic Peninsula. *Nat. Geosci.* **14**, 383–388 (2021).
- Kurtén, T., Loukonen, V., Vehkamäki, H. & Kulmala, M. Amines are likely to enhance neutral and ion-induced sulfuric acid-water nucleation in the atmosphere more effectively than ammonia. *Atmos. Chem. Phys.* **8**, 4095–4103 (2008).
- Almeida, J. et al. Molecular understanding of sulphuric acid-amine particle nucleation in the atmosphere. *Nature* **502**, 359–363 (2013).
- Meehl, G. A. et al. Sustained ocean changes contributed to sudden Antarctic sea ice retreat in late 2016. *Nat. Commun.* **10**, 14 (2019).
- Shepherd, A. et al. Mass balance of the Antarctic Ice Sheet from 1992 to 2017. *Nature* **558**, 219–222 (2018).
- Swadling, K. M. et al. Biological responses to change in Antarctic sea ice habitats. *Front. Ecol. Evol.* **10**, 1073823 (2023).
- Fretwell, P. T. & Trathan, P. N. Discovery of new colonies by Sentinel2 reveals good and bad news for emperor penguins. *Remote Sens. Ecol. Conserv.* **7**, 139–153 (2021).
- Abakumov, E. V. et al. Ornithogenic factor of soil formation in Antarctica: a review. *Eurasia Soil Sci.* **54**, 528–540 (2021).
- Zhu, R., Sun, J., Liu, Y., Gong, Z. & Sun, L. Potential ammonia emissions from penguin guano, ornithogenic soils and seal colony soils in coastal Antarctica: effects of freezing-thawing cycles and selected environmental variables. *Antarct. Sci.* **23**, 78–92 (2011).
- Blackall, T. D. et al. Ammonia emissions from seabird colonies. *Geophys. Res. Lett.* **34**, L10801 (2007).
- Theobald, M. R., Crittenden, P. D., Tang, Y. S. & Sutton, M. A. The application of inverse-dispersion and gradient methods to estimate ammonia emissions from a penguin colony. *Atmos. Environ.* **81**, 320–329 (2013).
- Ellis, R. A. et al. The influence of gas-particle partitioning and surface-atmosphere exchange on ammonia during BAQS-Met. *Atmos. Chem. Phys.* **11**, 133–145 (2011).
- Nair, A. A. & Yu, F. Quantification of atmospheric ammonia concentrations: a review of its measurement and modeling. *Atmosphere* **11**, 1092 (2020).
- Fretwell, P. Four unreported emperor penguin colonies discovered by satellite. *Antarct. Sci.* <https://doi.org/10.1017/S0954102023000329> (2024).
- Tian, R. et al. Freeze-thaw process boosts penguin-derived NH₃ emissions and enhances climate-relevant particles formation in Antarctica. *Npj Clim. Atmos. Sci.* **7**, 1–12 (2024).
- Schobesberger, S. et al. On the composition of ammonia–sulfuric acid ion clusters during aerosol particle formation. *Atmos. Chem. Phys.* **15**, 55–78 (2015).
- Dunne, E. M. et al. Global atmospheric particle formation from CERN CLOUD measurements. *Science* **354**, 1119–1124 (2016).
- Xiao, M. et al. The driving factors of new particle formation and growth in the polluted boundary layer. *Atmos. Chem. Phys.* **21**, 14275–14291 (2021).

38. Kürten, A. et al. New particle formation in the sulfuric acid–dimethylamine–water system: reevaluation of CLOUD chamber measurements and comparison to an aerosol nucleation and growth model. *Atmos. Chem. Phys.* **18**, 845–863 (2018).
39. Wu, L. et al. Molecular transformation of organic nitrogen in Antarctic penguin guano-affected soil. *Environ. Int.* **172**, 107796 (2023).
40. Dall'Osto, M. et al. Simultaneous Detection of Alkylamines in the Surface Ocean and Atmosphere of the Antarctic Sympagic Environment. *ACS Earth Space Chem.* **3**, 854–862 (2019).
41. Dall'Osto, M. et al. Antarctic sea ice region as a source of biogenic organic nitrogen in aerosols. *Sci. Rep.* **7**, 1–10 (2017).
42. Paglione, M. et al. Simultaneous organic aerosol source apportionment at two Antarctic sites reveals large-scale and ecoregion-specific components. *Atmos. Chem. Phys.* **24**, 6305–6322 (2024).
43. Saiz-Lopez, A., Blaszczyk-Boxe, C. S. & Carpenter, L. J. A mechanism for biologically induced iodine emissions from sea ice. *Atmos. Chem. Phys.* **15**, 9731–9746 (2015).
44. Kim, J. et al. New particle formation events observed at King Sejong Station, Antarctic Peninsula – Part 1: physical characteristics and contribution to cloud condensation nuclei. *Atmos. Chem. Phys.* **19**, 7583–7594 (2019).
45. Kecorius, S. et al. Rapid growth of Aitken-mode particles during Arctic summer by fog chemical processing and its implication. *PNAS Nexus* **2**, pgad124 (2023).
46. Lana, A. et al. An updated climatology of surface dimethylsulfide concentrations and emission fluxes in the global ocean. *Glob. Biogeochem. Cycles* **25**, GB1004 (2011).
47. Hulswar, S. et al. Third revision of the global surface seawater dimethyl sulfide climatology (DMS-Rev3). *Earth Syst. Sci. Data* **14**, 2963–2987 (2022).
48. Adams, P. J., Seinfeld, J. H. & Koch, D. M. Global concentrations of tropospheric sulfate, nitrate, and ammonium aerosol simulated in a general circulation model. *J. Geophys. Res. Atmos.* **104**, 13791–13823 (1999).
49. Pye, H. O. T. et al. Effect of changes in climate and emissions on future sulfate-nitrate-ammonium aerosol levels in the United States. *J. Geophys. Res. Atmos.* **114**, D01205 (2009).
50. Kyrö, E.-M. et al. Antarctic new particle formation from continental biogenic precursors. *Atmos. Chem. Phys.* **13**, 3527–3546 (2013).
51. Trathan, P. N. et al. The emperor penguin—vulnerable to projected rates of warming and sea ice loss. *Biol. Conserv.* **241**, 108216 (2020).
52. Fretwell, P. T., Boutet, A. & Ratcliffe, N. Record low 2022 Antarctic sea ice led to catastrophic breeding failure of emperor penguins. *Commun. Earth Environ.* **4**, 1–6 (2023).
53. Jenouvrier, S. et al. The call of the emperor penguin: legal responses to species threatened by climate change. *Glob. Change Biol.* **27**, 5008–5029 (2021).
54. Baccarini, A. et al. Low-volatility vapors and new particle formation over the southern ocean during the antarctic circumnavigation expedition. *J. Geophys. Res. Atmos.* **126**, e2021JD035126 (2021).
55. Jorga, S. D., Florou, K., Patoulas, D. & Pandis, S. N. New particle formation and growth during summer in an urban environment: a dual chamber study. *Atmos. Chem. Phys.* **23**, 85–97 (2023).
56. Aktipis, A. et al. Infrequent new particle formation in a coastal Mediterranean city during the summer. *Atmos. Environ.* **302**, 119732 (2023).
57. Aktipis, A. et al. Significant spatial gradients in new particle formation frequency in Greece during summer. *Atmos. Chem. Phys.* **24**, 65–84 (2024).
58. Dada, L. et al. The synergistic role of sulfuric acid, ammonia and organics in particle formation over an agricultural land. *Environ. Sci. Atmos.* **3**, 1195–1211 (2023).
59. Altieri, K. E., Spence, K. A. M. & Smith, S. Air-sea ammonia fluxes calculated from high-resolution summertime observations across the Atlantic Southern Ocean. *Geophys. Res. Lett.* **48**, e2020GL091963 (2021).
60. Asmi, E. et al. Primary sources control the variability of aerosol optical properties in the Antarctic Peninsula. *Tellus B Chem. Phys. Meteorol.* **70**, 1414571 (2018).
61. Perchivale, P. J. et al. Updated estimate of the breeding population of Adélie penguins (*Pygoscelis adeliae*) at Penguin Point, Marambio/ Seymour Island within the proposed Weddell Sea Marine Protected Area. Preprint at *arXiv* <https://doi.org/10.21203/rs.3.rs-2117503/v1> (2022).
62. Lynch, H. J. & LaRue, M. A. First global census of the Adélie Penguin. *The Auk* **131**, 457–466 (2014).
63. Lynch, H. J., Naveen, R. & Casanovas, P. Antarctic Site Inventory breeding bird survey data, 1994–2013. *Ecology* **94**, 2653–2653 (2013).
64. Ellis, R. A. et al. Characterizing a quantum cascade tunable infrared laser differential absorption spectrometer (QC-TILDAS) for measurements of atmospheric ammonia. *Atmos. Meas. Tech.* **3**, 397–406 (2010).
65. Moravek, A., Singh, S., Pattey, E., Pelletier, L. & Murphy, J. G. Measurements and quality control of ammonia eddy covariance fluxes: a new strategy for high-frequency attenuation correction. *Atmos. Meas. Tech.* **12**, 6059–6078 (2019).
66. Jokinen, T. et al. Atmospheric sulphuric acid and neutral cluster measurements using CI-API-TOF. *Atmos. Chem. Phys.* **12**, 4117–4125 (2012).
67. Rissanen, M. P., Mikkilä, J., Iyer, S. & Hakala, J. Multi-scheme chemical ionization inlet (MION) for fast switching of reagent ion chemistry in atmospheric pressure chemical ionization mass spectrometry (CIMS) applications. *Atmos. Meas. Tech.* **12**, 6635–6646 (2019).
68. Kürten, A., Rondo, L., Ehrhart, S. & Curtius, J. Calibration of a chemical ionization mass spectrometer for the measurement of gaseous sulfuric acid. *J. Phys. Chem. A* **116**, 6375–6386 (2012).
69. Mirme, S. & Mirme, A. The mathematical principles and design of the NAIS—a spectrometer for the measurement of cluster ion and nanometer aerosol size distributions. *Atmos. Meas. Tech.* **6**, 1061–1071 (2013).
70. Manninen, H. E., Mirme, S., Mirme, A., Petäjä, T. & Kulmala, M. How to reliably detect molecular clusters and nucleation mode particles with Neutral cluster and Air Ion Spectrometer (NAIS). *Atmos. Meas. Tech.* **9**, 3577–3605 (2016).
71. Aalto, P. et al. Physical characterization of aerosol particles during nucleation events. **53**, 344–358 (2001).
72. Winklmayr, W., Reischl, G. P., Lindner, A. O. & Berner, A. A new electromobility spectrometer for the measurement of aerosol size distributions in the size range from 1 to 1000 nm. *J. Aerosol Sci.* **22**, 289–296 (1991).
73. Roberts, G. C. & Nenes, A. A continuous-flow streamwise thermal-gradient CCN chamber for atmospheric measurements. *Aerosol Sci. Technol.* **39**, 206–221 (2005).
74. Fröhlich, R. et al. The ToF-ACSM: a portable aerosol chemical speciation monitor with TOFMS detection. *Atmos. Meas. Tech.* **6**, 3225–3241 (2013).
75. Möhler, O. et al. The Portable Ice Nucleation Experiment (PINE): a new online instrument for laboratory studies and automated long-term field observations of ice-nucleating particles. *Atmos. Meas. Tech.* **14**, 1143–1166 (2021).
76. Kulmala, M. et al. Measurement of the nucleation of atmospheric aerosol particles. *Nat. Protoc.* **7**, 1651–1667 (2012).
77. Asmi, E. et al. Results of the first air ion spectrometer calibration and intercomparison workshop. *Atmos. Chem. Phys.* **9**, 141–154 (2009).
78. Kangasluoma, J. et al. Overview of measurements and current instrumentation for 1–10 nm aerosol particle number size distributions. *J. Aerosol Sci.* **148**, 105584 (2020).

Acknowledgements

This work was supported by the Research Council of Finland project funding via ACFA grant #335844, #335845, and #333397; the Atmosphere and Climate Competence Center (ACCC) Flagship support from the Research Council of Finland (337549, 357902, 359340 for the University of Helsinki and 337552, 357904, 359342 for the Finnish Meteorological Institute); by European Union (FOCI (Non-CO₂ forcers and their climate, weather, air quality and health impacts, agreement no. 101056783); and the European Union's Horizon 2020 research and innovation program under CRICES (Climate Relevant interactions and feedbacks: the key role of sea ice and Snow in the polar and global climate system) grant agreement No. 101003826. We thank Aerodyne Research Inc. for loaning an ammonia instrument, and wish to acknowledge Kenji Lizardo, Carolyn Fialkowski, and Ruth Heckbert for logistical support. We thank Palas GmbH for lending instrumentation, and particularly Ann-Kathrin Gossmann for her assistance in the field deployment. We also wish to thank the on-site support from the Argentinian Servicio Meteorológico Nacional team at the Pabellón Científico, including Daniel Sofiev-Rios, Gabriel Arias, and Facundo Penayo. We also thank the Dirección Nacional del Antártico (DNA). Finally, we acknowledge the logistical support from FINNARP, the Fuerza Aérea Argentina, the Comando Conjunto Antártico (COCOANTAR), and all other support personnel at Marambio Station.

Author contributions

M.B., L.Q., Z.B., S.S.-R., G.M., and F.Q. executed the field campaign. M.B., L.Q., Z.B., and B.M. analyzed the data. M.B. wrote the paper with L.Q., Z.B., V.K., D.W., M.S., and X.H. B.M., S.H., M.Ag., J.R., D.N., R.R., F.W., S.S., H.T., M.Au, L.B., C.X., and A.B. provided insight on the operation, analysis, and interpretation of datasets and instrumentation. P.P. gave insights and observations on penguin/seabird populations. L.Q., G.M., F.Q., M.B., Z.B., S.S.-R., A.V., E.A., and M.S. planned and coordinated the field campaign. E.A. oversees the installation, maintenance, and upkeep of the site instrumentation and infrastructure. D.W., M.S., M.K., and T.P. conceived the idea for the paper. All authors commented on and approved of the final version of the paper.

Competing interests

The authors declare no competing interests.

Additional information

Supplementary information The online version contains supplementary material available at <https://doi.org/10.1038/s43247-025-02312-2>.

Correspondence and requests for materials should be addressed to Matthew Boyer or Mikko Sipilä.

Peer review information *Communications Earth & Environment* thanks the anonymous reviewers for their contribution to the peer review of this work. Primary Handling Editors: Keiichiro Hara and Alice Drinkwater. A peer review file is available.

Reprints and permissions information is available at <http://www.nature.com/reprints>

Publisher's note Springer Nature remains neutral with regard to jurisdictional claims in published maps and institutional affiliations.

Open Access This article is licensed under a Creative Commons Attribution 4.0 International License, which permits use, sharing, adaptation, distribution and reproduction in any medium or format, as long as you give appropriate credit to the original author(s) and the source, provide a link to the Creative Commons licence, and indicate if changes were made. The images or other third party material in this article are included in the article's Creative Commons licence, unless indicated otherwise in a credit line to the material. If material is not included in the article's Creative Commons licence and your intended use is not permitted by statutory regulation or exceeds the permitted use, you will need to obtain permission directly from the copyright holder. To view a copy of this licence, visit <http://creativecommons.org/licenses/by/4.0/>.

© The Author(s) 2025